

## Article

# Assessment and Prediction of the Water Quality Index for the Groundwater of the Ghiss-Nekkor (Al Hoceima, Northeastern Morocco)

Yassine El Yousfi <sup>1</sup>, Mahjoub Himi <sup>1,2</sup>, Hossain El Ouarghi <sup>1</sup>, Mourad Aqnouy <sup>3</sup>, Said Benyoussef <sup>1,4</sup>, Hicham Gueddari <sup>5</sup>, Hanane Ait Hmeid <sup>5</sup>, Abdennabi Alitane <sup>6,7,\*</sup>, Mohamed Chaibi <sup>8</sup>, Muhammad Zahid <sup>9,10</sup>, Narjisse Essahlaoui <sup>6</sup>, Sliman Hitouri <sup>11</sup>, Ali Essahlaoui <sup>6</sup> and Abdallah Elaaraaj <sup>12,13</sup>

- <sup>1</sup> Environmental Management and Civil Engineering Team, ENSAH, Abdelmalek Essaadi University, Tetouan 93030, Morocco
  - <sup>2</sup> Faculty of Geology, University of Barcelona, Marti I Franques S/N, 08028 Barcelona, Spain
  - <sup>3</sup> Applied Geology and Remote Sensing Research Team, Applied Geology Research Laboratory, Faculty of Sciences and Techniques, Moulay Ismail University of Meknes, Errachidia 52000, Morocco
  - <sup>4</sup> Research Team: Biology, Environment and Health, Department of Biology, Errachidia Faculty of Science and Technology, University of Moulay Ismail, Meknes 50000, Morocco
  - <sup>5</sup> OLMAN BPGE Laboratory, Multidisciplinary Faculty of Nador, Mohamed First University, Oujda 60000, Morocco
  - <sup>6</sup> Research Group “Water Sciences and Environment Engineering”, Geoengineering and Environment Laboratory, Geology Department, Faculty of Sciences, Moulay Ismail University, Presidency, Marjane 2, P.O. Box 298, Meknes 50050, Morocco
  - <sup>7</sup> Hydrology and Hydraulic Engineering Department, Vrije Universiteit Brussels (VUB), 1050 Brussels, Belgium
  - <sup>8</sup> Team of Renewable Energy and Energy Efficiency, Department of Physics, Faculty of Science, University of Moulay Ismail, Zitoune, P.O. Box 11201, Meknes 50050, Morocco
  - <sup>9</sup> Key Laboratory of Functional Inorganic Material Chemistry, Ministry of Education of the People’s Republic of China, Heilongjiang University, Harbin 150080, China
  - <sup>10</sup> School of Natural Sciences, National University of Science and Technology, Islamabad 44000, Pakistan
  - <sup>11</sup> Geosciences Laboratory, Department of Geology, Faculty of Sciences, University Ibn Tofail, P.O. Box 133, Kenitra 14000, Morocco
  - <sup>12</sup> Natural Resources and Environment Laboratory, Geology Department, Polydisciplinary Faculty of Taza, Route d’Oujda, P.O. Box 1223, Taza 35000, Morocco
  - <sup>13</sup> Engineering Sciences and Techniques Center, Environment Department, Faculty of Science and Technology, Sidi Mohamed Ben Abdellah University of FEZ, P.O. Box 2202, Fes 30000, Morocco
- \* Correspondence: [abdennabi.alitane@vub.be](mailto:abdennabi.alitane@vub.be)



**Citation:** El Yousfi, Y.; Himi, M.; El Ouarghi, H.; Aqnouy, M.; Benyoussef, S.; Gueddari, H.; Ait Hmeid, H.; Alitane, A.; Chaibi, M.; Zahid, M.; et al. Assessment and Prediction of the Water Quality Index for the Groundwater of the Ghiss-Nekkor (Al Hoceima, Northeastern Morocco). *Sustainability* **2023**, *15*, 402. <https://doi.org/10.3390/su15010402>

Academic Editors: Quoc Bao Pham, Antonietta Varasano and Meriame Mohajane

Received: 15 October 2022  
Revised: 11 December 2022  
Accepted: 21 December 2022  
Published: 26 December 2022



**Copyright:** © 2022 by the authors. Licensee MDPI, Basel, Switzerland. This article is an open access article distributed under the terms and conditions of the Creative Commons Attribution (CC BY) license (<https://creativecommons.org/licenses/by/4.0/>).

**Abstract:** Water quality index (WQI) is the primary method applied to characterize water quality in the world. The current study employed the statistical analysis and multilayer perceptron (MLP) approaches for predicting groundwater quality in the Ghiss-Nekkor aquifer, northeast of Al Hoceima, Morocco. Fifty sampled groundwater were identified and analyzed for major anions and cations throughout May 2019. Several physicochemical parameters of all the samples were identified in this investigation, such as TDS, pH, EC, Na, K, Ca, Mg, HCO<sub>3</sub>, NO<sub>3</sub>, Br, SO<sub>4</sub>, and Cl. The entropy-weighted groundwater quality index (EWQI) was calculated from these parameters. The WQI procedure determined the suitability of groundwater for consumption. The WQI value varied from 90.98 to 337.28. The EC, TDS, WQI, and Cl<sup>−</sup> spatial distribution showed that EC and Cl<sup>−</sup> are associated with poor groundwater quality. A single sample (W16) represented unsuitable water for drinking purposes and offered a WQI value of 337.28, indicating poor drinking quality due to seawater intrusion, overexploitation, and harsh weather conditions. The majority of the values obtained for the parameters exceeded the recommended limit of the World Health Organization (WHO)’s guidelines for consumption. The findings show that using parameters is a straightforward method for predicting water quality indexes with sufficient and suitable precision. The MLP model shows good predictive performances in terms of the coefficient of determination R<sup>2</sup>, mean absolute error (MAE), and root-mean-square error (RMSE) with values of 0.9885, 5.8031, and 4.7211, respectively. The ANN approach was applied to develop a model that can accurately predict WQI utilizing mineralization, TH, NO<sub>3</sub>, and NO<sub>2</sub> as inputs. The MAE for the model’s performance was calculated to be 4.72. A Bland–Altman

test was used to validate that the model is suitable. Following the test, it was determined that the model is appropriate for predicting WQI, with an error of just 0.1%.

**Keywords:** groundwater quality; prediction; water quality index; Ghiss-Nekkor; WHO; artificial neural network

---

## 1. Introduction

Groundwater is a significant source of drinking water for the benefit of people around the world; it also meets a substantial portion of agricultural and domestic demand [1]. Water quality is determined by biological and physico-chemical parameters [2]. These variables are essential to evaluate water quality, including for potable water, before using it, for numerous reasons. Although human influences exist in many nations, water quality is a sensitive and critical issue. Water quality is intimately tied to human health; thus, water is exposed to gradual and severe contamination, so it is also necessary to investigate wastewater quality before discharge and to establish a cost-effective technology of controlling and preventing groundwater pollution [3–5]. Consequently, monitoring water characteristics to maintain water quality is critical [6]. In addition, pollution is caused by human activities, leading to a decrease in the quality of groundwater and its use as well as the water quality and water quantity of groundwater in recent decades [7–11]. For the efficient management and planning of groundwater resources, groundwater vulnerability assessment is critical [12].

Across many circumstances, using this approach enables the appropriate identification of contaminated sites and may be required for legal-compliance checks. At present, water quality management is highlighted as a significant and significant challenge, particularly the identification of point and non-point contaminant sources in the Ghiss-Nekkor aquifer. Consequently, water quality management does not readily provide an accurate overall perspective of the temporal and spatial trends in the global quality of water in an aquifer, except for several attempts to generate a comprehensive methodology that significantly combines data sources and renders them into practical information. As a result, it is critical to provide innovative ways to analyze and, if feasible, forecast water quality (WQ).

The water quality index (WQI) proposed by [13] is a subjective method for assessing the consumption appropriateness of surface water and groundwater quality that has been frequently utilized in research [14–16]. We employed the groundwater quality index (GWQI), firstly applied by [17], to evaluate groundwater quality.

ANNs provide an attractive solution for simulating the water resources system [18,19]. Multiple investigations have been carried out on applying neural networks to the forecasting of groundwater [20,21]. The multilayer perceptron (MLP) model is the most famous tool used in environment forecasting due to its high predictive capability and handling of nonlinear relationships. Therefore, the WQI is an effective instrument for assessing water quality, and it has been used in numerous studies by academics and researchers [22–26]. The objective of this paper was to study and identify the WQI level in 50 groundwater wells in the Ghiss-Nekkor aquifer, assessing the quality of groundwater for drinking water by using Schuler and Wilcox diagrams, and, by determining the WQI, develop the MLP model for WQI prediction. A neural network was used to predict the WQI before and after the monsoon in India's Shivganga River basin. The network had 13 parameters, six hidden neurons, and one output, WQI. From this point, we innovated the work approach by establishing a distinct model for pre- and post-monsoon, adding temporal WQI variation, and lowering inputs. ANN has not been used to create the WQI temporal and spatial prediction method for the Ghiss-Nekkor. The current research aimed to determine the performance of groundwater suitable for drinking by computing WQI with 13 parameters, then reduce the number of variables involved in WQI prediction using PCA, and develop an ANN model capable of predicting WQI temporal and spatial variation with the fewest possible inputs.

The principal objectives of this paper were to identify and evaluate the suitability of groundwater in the Ghiss-Nekkor plain, potentially for drinking and irrigation, by calculating the WQI in 50 wells with specific importance weights and to validate the relevance of the indices by comparing them with other approaches to quality assessment. Additionally, the purpose of this work was to identify areas with sufficient water quality for irrigation and drinking for efficient management of groundwater supplies in the survey area.

## 2. Materials and Methods

### 2.1. Study Area Description

The study area is situated between  $35^{\circ}3.53'$  to  $35^{\circ}15.05'$  N latitude and  $3^{\circ}55.11'$  to  $3^{\circ}45.42'$  W longitude in Al Hoceima Province (Figure 1), which is located in northeastern Morocco. The covered area of the study plain is approximately 100 km<sup>2</sup> [27]. Due to the variable precipitation and high potential evapotranspiration in the Ghiss-Nekkor aquifer's climate, even if there is a slight surplus [28], it is inadequate to make up for the hydric shortage.

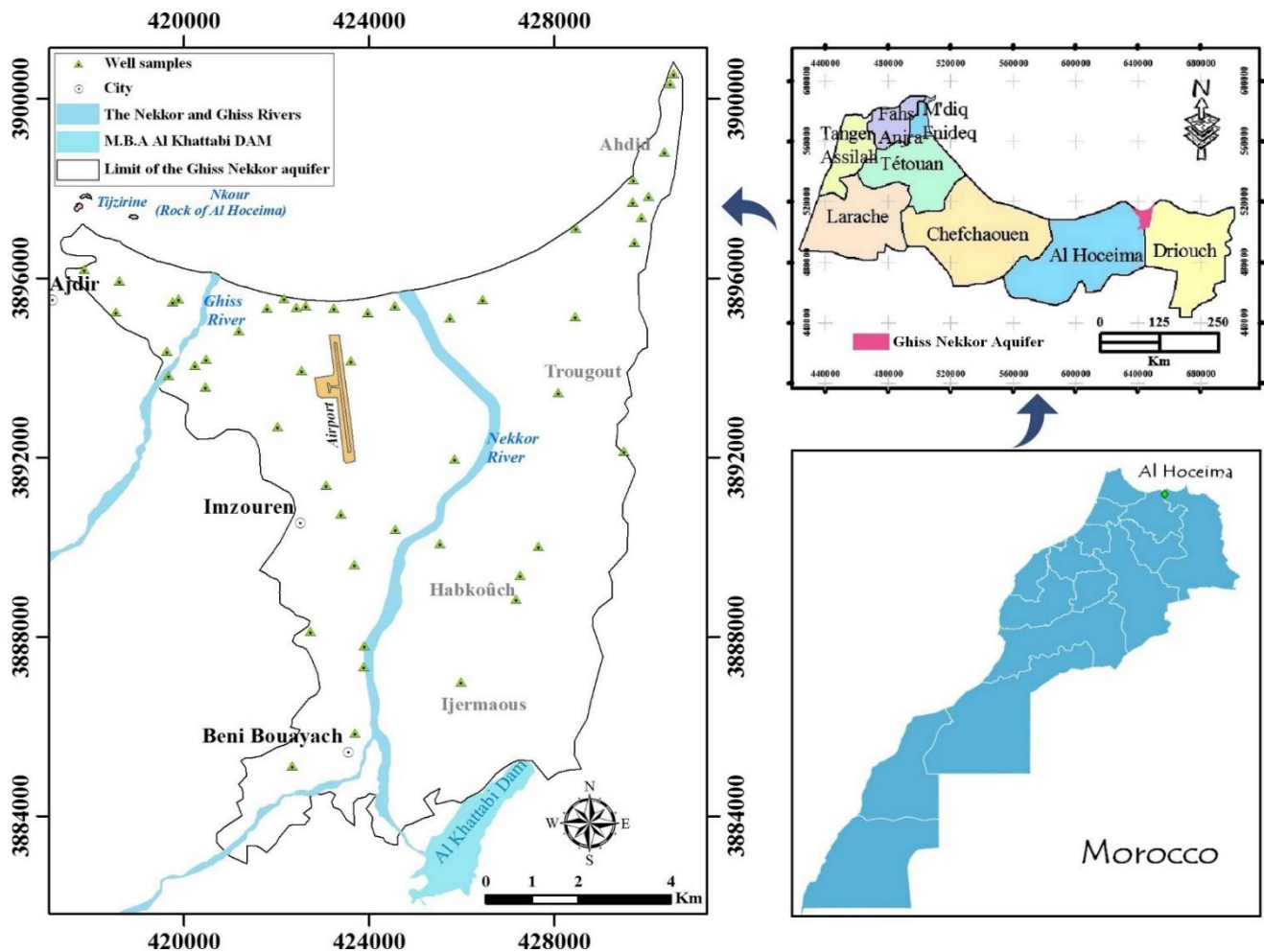


**Figure 1.** Study area and location of wells for drinking water in the Ghiss-Nekkor aquifer.

### 2.2. Geology Setting

The aquifer of Ghiss-Nekkor belongs to the structural domain of the Rif. It constitutes the transition zone between the central and eastern Rif, with main geological terrains that present distinct units often separated by thrust faults. The Ghiss-Nekkor plain is bound by the Trougout and Bousekkor-Aghbal onshore fault, covering the offshore of the Mediterranean Sea [29]). To the west of the coastal fringe of Al Hoceima, the internal

zones are represented by the Bokkoya massif. The Bokkoya fault is a significant easterly dipping fault, which bounds the western side of Al Hoceima Bay [30]. The flysch zones are represented by the Tisiréne unit, and the intrarif (external metamorphosed zones) is marked by the Ketama unit. To the east of the bay, on the other side of the Nekkour plain, the E–W extension of the units is affected by the Nekkour major accident. This accident marks the transition between the external Rif units, Ketama and Temsamane [31]. In addition, there is the Neogene volcanic massif of Ras Tarf, constituting the Temsamane borders of the Boudinar basin. Toward the north, the region of Al Hoceima is delimited by the Alboran marine domain, and the main geological and tectonic structure in this zone is the Alboran wrinkle.

The current study includes a diversity of alluvial geological formations consisting mainly of recent and present middle quaternary age (sands, gravels, silts, clays, and pebbles) [32], supported by a substratum of primary quartzites, blue schistose marls, and silts of middle and ancient quaternary age [33]. Therefore, the stratigraphy of the Ghiss-Nekkour Plain covers a depression filled by sediments ranging from Plio-Villafranchian to recent Quaternary. Nekkour river plain silts, on the other hand, are responsible for the recent Quaternary sediments. The thickness of the Quaternary formations generally exceeds 100 m deep and reaches 450 m east of Imzourene [34].

### 2.3. Methodology

The samples of water in this study were taken in clean polyethylene bottles. At each sampling time, the bottles were rinsed thoroughly two to three times with the groundwater to be sampled, and water samples were collected after pumping for 10 min. At the time of sampling, there were some in situ measures that included temperature, electrical conductivity (EC), TDS, and pH, which were measured using a multiparameter device (HANA HI 98194) that has an accuracy of  $\pm 0.01$  units for pH and  $\pm 1\%$  (or  $\pm 1 \mu\text{S}/\text{cm}$ ) for electrical conductivity [34]. For analysis of major cations and anions, groundwater was filtered in the field using a syringe and 0.45  $\mu\text{m}$  membrane filters. Sampling was conducted according to Rodier's protocol [35]. Potassium  $\text{K}^+$  and Sodium  $\text{Na}^+$  were measured with a CL 361 flame photometer at the LSA-GE2 laboratory of ENSA, Al Hoceima. Nitrate  $\text{NO}_3^-$  was measured with a HACH LANGE DR 1900, and Sulfate  $\text{SO}_4^{2-}$  was measured with a Shimadzu UV-1800 spectrophotometer. Chloride  $\text{Cl}^-$  was determined by the titration method 0.05N  $\text{AgNO}_3$ . Magnesium concentration  $\text{Mg}^{2+}$  was calculated using the following method: Magnesium hardness = total hardness—Calcium hardness  $\text{Mg}^{2+}$  (mg/L) =  $\text{MgH} \times \text{Mg}^{2+}$  equivalent weight  $\times$  EDTA normality. Calcium hardness  $\text{Ca}^{2+}$  and total hardness (TH as  $\text{CaCO}_3$ ) were determined by the EDTA titration method. Using a standard 0.01N sulfuric acid solution ( $\text{H}_2\text{SO}_4$ ) and a methyl orange indicator, the bicarbonate concentration was determined for  $\text{HCO}_3^-$ . Using ion-selective electrodes, the  $\text{Br}^-$  concentration of the groundwater was analyzed (Orion Bromide 9635BNWP electrode), which was investigated by the Technical and Scientific Services of the University of Barcelona [36]. Standard solutions were used to confirm the accuracy of the approaches. The estimated analytical errors were between 5% and 10% [36].

The results obtained were presented in the form of thematic maps prepared with ArcGIS software. The methods used for the analysis of the different physico-chemical parameters used in this study are essentially those described in Figure 2.

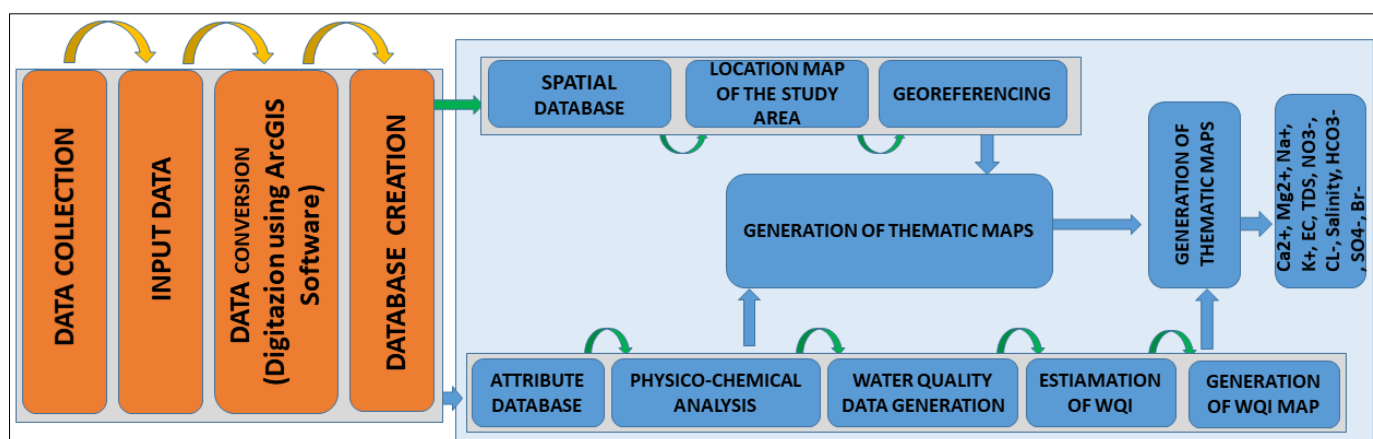


Figure 2. Methodology performed in the study.

#### 2.4. Sampling and Analysis Protocol of Groundwater

A total of 50 samples of groundwater were collected from domestic, irrigation, and industrial wells in the Ghiss-Nekkor aquifer during May 2019 (Supplementary Table S3). The same survey dataset included 13 groundwater quality variables (pH, T, TDS, EC, Ca, Mg, Na, K, NO<sub>3</sub>, HCO<sub>3</sub>, Cl, Br, and SO<sub>4</sub>) (Table 1). Groundwater samples were collected in high-density polyethylene bottles (HDPE) after double rinsing with distilled water. Groundwater samples were conserved in an icebox and brought to the laboratory for chemical analysis; the pieces were refrigerated at a temperature of 4 °C until the subsequent analysis of parameters. The pH was measured on site with a pH meter. Global positioning was also recorded for each sampling location. All the sampling, transport, and storage procedures followed the standard method recommended by the World Health Organization [2]. Statistical analyses and data processing were performed using software (Surfer 13, ArcGis 10.5, and Grapher 14) (Figure 3).

Table 1. Statistical description of groundwater quality variables for Ghiss-Nekkor sampling wells.

Groundwater Quality Variables	Min	Max	Average	Median	St. Dev.
TDS (mg/L)	1130	5035	2323.92	2136.5	885.66
pH	6.59	8.01	7.33	7.36	0.34
T (°C)	7.91	25.27	18.52	20.54	4.49
EC (µS/cm)	2280	10,070	4646.14	4273.5	1778.42
Na (mg/L)	214.5	954	404.53	397.75	160.05
K (mg/L)	1.7	45.3	7.54	4.5	7.55
NO <sub>3</sub> (mg/L)	0.9	79.9	10.16	7.15	11.83
HCO <sub>3</sub> (mg/L)	256.2	744.2	390.34	382.78	83.62
Ca (mg/L)	124.25	400.8	232.87	216.43	68.11
Mg (mg/L)	53.76	254	140.37	130.56	46.25
Cl (mg/L)	213	2698	907.03	834.25	472.67
SO <sub>4</sub> (mg/L)	64.62	1514.34	597.09	544.93	327.04
Br (mg/L)	1.94	5.33	3.17	3.11	0.71
SAR	3.14	11.6	5.22	4.82	1.91
RSC	−30.74	−4.61	−16.78	−16.00	6.29
Salinity	1.18	5.35	2.47	2.34	0.96

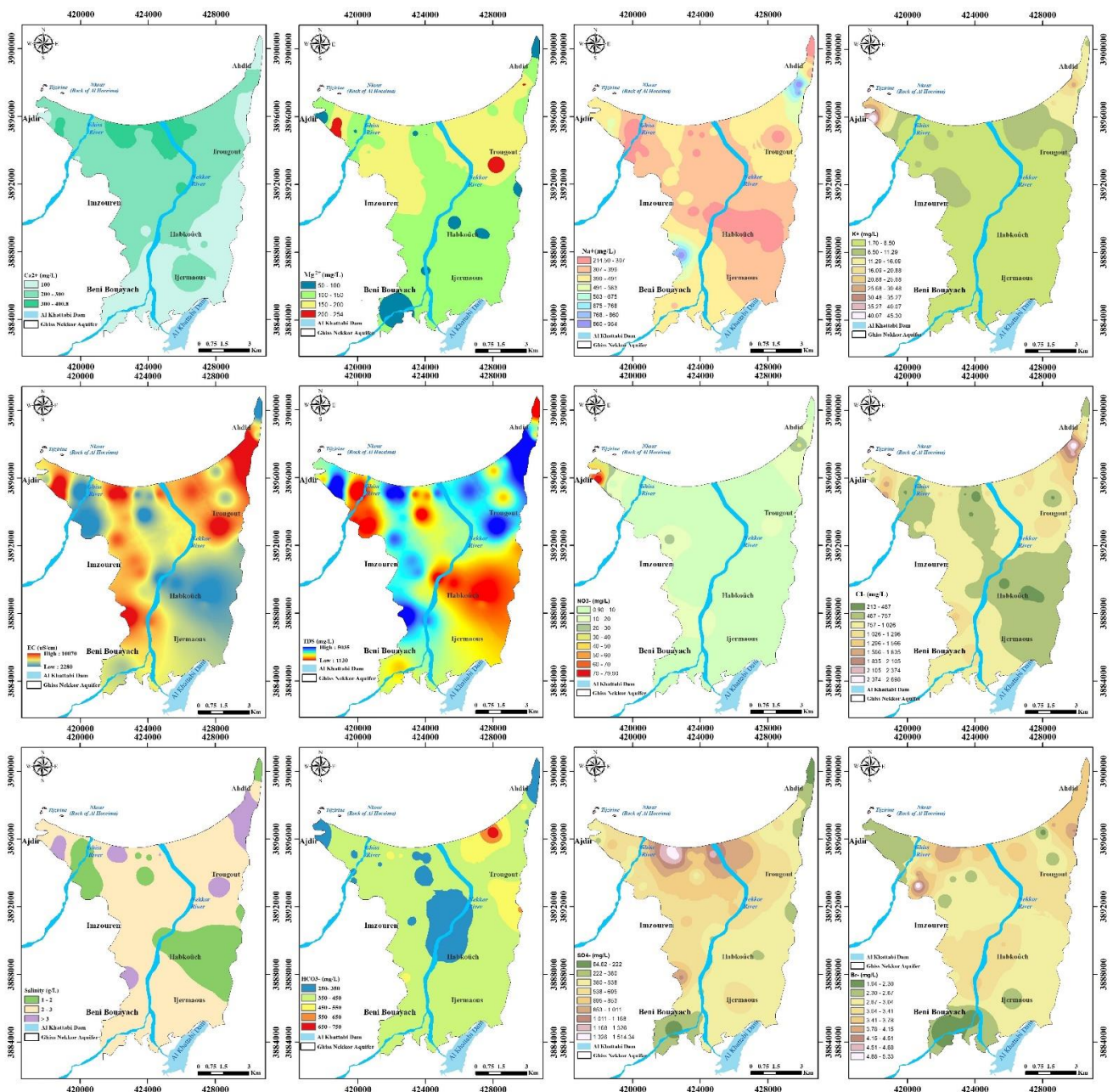


**Figure 3.** Distribution of major element concentrations in groundwater in the study area ( $\text{Ca}^{2+}$ ,  $\text{Mg}^{2+}$ , EC, TDS, salinity,  $\text{HCO}_3^-$ ,  $\text{Na}^+$ ,  $\text{K}^+$ ,  $\text{NO}_3^-$ ,  $\text{Cl}^-$ ,  $\text{Br}^-$ , and  $\text{SO}_4^{2+}$ ).

The statistical methodology is mainly based on principal component analysis (PCA) to investigate the phenomena responsible for the water mineralization. Statistical analyses were performed with SPSS and XLSTAT software. The parameter values are compared to the World Health Organization (WHO).

### 2.5. Water Quality Index Method

A water quality index is a simple tool for determining water quality [37–41]. It is a value-based approach for representing the total quality of groundwater. The quality of groundwater is essential because it determines the appropriateness of water for drinking [42]. It provides an efficient method of interpreting water quality by combining different parameters into a single number [43,44]. The WQI in this study is defined using chemical analyses of groundwater in the Ghiss-Nekkor aquifer. In most cases, four steps are taken to

generate WQI by considering many parameters. The weightage ( $w_i$ ) of the 13 parameters ( $\text{Na}^+$ , T,  $\text{K}^+$ , EC, pH, TDS,  $\text{SO}_4^-$ ,  $\text{HCO}_3^-$ ,  $\text{Ca}^{2+}$ ,  $\text{Mg}^{2+}$ ,  $\text{Br}^-$ ,  $\text{Cl}^-$ , and  $\text{NO}_3^-$ ) was provided in the first step by evaluating its rank in investigating the quality of water for human consumption. Used to determine WQI, the [45] drinking utility ranges must be considered.

$$W_i = w_i / \sum_{i=1}^n w_i \quad (1)$$

Each parameter has a unit weight of  $W_i$ , and  $n$  is the number of parameters. The quality rating scale ( $q_i$ ) for each parameter is computed by dividing the concentration in each water sample by the attention in the applicable WHO guidelines [45]. Finally, the result is multiplied by 100 by using the formula.

$$q_i = \left( \frac{C_i}{S_i} \right) \times 100 \quad (2)$$

Initially, the WQI is calculated by giving each of the measured parameters a value between 1 and 5 on a scale of significance ( $w_i$ ) (Table 2).

**Table 2.** Weight and relative weight of each parameter [46,47].

Symbol	Drinking Water			Irrigation Water		
	Si (WHO 2011)	(wi)	(Rwi)	Si (Ayers and Westcot 1985)	(wi)	(Rwi)
EC ( $\mu\text{S}/\text{cm}$ )	1500	5	0.135	2500	5	0.109
TDS (mg/L)	1000	5	0.135	1000	5	0.109
pH	6.5–9.5	3	0.081	8.5	4	0.087
$\text{HCO}_3^-$ (mg/L)	300	1	0.027	400	2	0.043
$\text{SO}_4^{2-}$ (mg/L)	250	4	0.108	250	5	0.109
$\text{Cl}^-$ (mg/L)	250	4	0.108	350	5	0.109
$\text{Na}^+$ (mg/L)	200	3	0.081	200	5	0.109
$\text{K}^+$ (mg/L)	12	3	0.081	10	3	0.064
$\text{NO}_3^-$ (mg/L)	50	5	0.135	50	2	0.043
$\text{Ca}^{2+}$ (mg/L)	200	2	0.054	200	5	0.109
$\text{Mg}^{2+}$ (mg/L)	150	2	0.054	100	5	0.109
Total		37	1.00		46	1.00

$Q_i$  is the quality rating,  $C_i$  refers to the concentration of each chemical parameter in each sample (mg/L), and  $S_i$  refers to the standard limit for each chemical parameter (mg/L) given by guidelines of the WHO for each chemical parameter in milligrams per liter. To generate the water quality index, calculate the  $S_i$  value for each parameter using the following equation.

$$S_i = W_i \times q_i \quad (3)$$

$$\text{WQI} = \sum_{i=1}^n S_i \quad (4)$$

$S_i$  indicates the subindex of the parameter, where  $q_i$  means the rating depending on the concentration of its parameter, and  $n$  is the number of parameters [16]. Furthermore, the WQI was calculated using the following formula.

The WQI is determined using GIS by interpolation. The map that results may be classified as having excellent water when lower than 50, good water in the range of 50–100, poor water in the range of 100–200, inferior water in the range of 200–300, and unsuitable water for drinking purposes when more than 300 [48,49].

## 2.6. Multilayer Perceptron (MLP)

MLP model is a kind of feedforward artificial neural network (Figure 4), with a design that has been inspired by the functioning of a biological neuron. The structure of an MLP

network consists of an input layer that distributes the input attributes to the first hidden layer, one or several hidden layers, and an output layer that receives the signal from the last hidden layer. Figure 4 depicts the structure of an MLP model with one hidden layer.

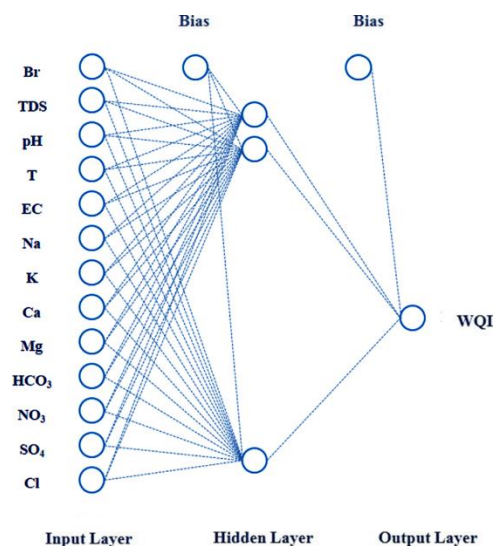


**Figure 4.** A multi-layer feed-forward artificial neural network model's structure.

The MLP model is a data-driven algorithm that seeks to find the relationship between the input vector  $x$  and the output vector  $y$  based on a dataset  $\{x_i, y_i\}_{i=1}^N$ , where  $N$  is the number of observations. In this paper, the input vector  $x$  is a matrix with 13 variables, namely: Br, TDS, pH, T, EC, Na, K, Ca, Mg,  $\text{HCO}_3$ ,  $\text{NO}_3$ ,  $\text{SO}_4$ , and Cl. However, the output vector  $y$  is the water quality index WQI.

The MLP model first moves the input data from the input layer via the hidden layer to the output layer. Then, the error is calculated and returned to the input layer. This strategy is repeated by adjusting the parameters of the model (weights and bias) by a learning algorithm until the mean squared error (MSE) reaches an acceptable level. MSE is defined by:

$$\text{MSE} = \frac{1}{N} \sum_{i=1}^N (\hat{y}_i - y_i)^2 \quad (5)$$

where  $\hat{y}_i$  is the estimated output by the MLP model. More details about the MLP model can be found in [50,51].

### 3. Results and Discussion

#### 3.1. Water Quality Index

The findings of a WQI are consistently related to the water-quality-language categories, and the assignment of a water quality rating for numerous reasons is fraught with ambiguity. The computed WQI concentration ranges from 90.98 to 337.28 (Figure 5). The samples' water quality indexes are shown in Table 3. There were 6% "good water" samples, 72% "poor water" samples, 20% "inferior water" samples, and 2% "water unfit for drinking purposes" samples in the Ghiss-Nekkor aquifer (Table 3).

This could be due to ion discharge, coastal zone development, seawater intrusion, agricultural input contamination, human waste, or sewage from homes and septic tanks, among other things (Table 3) [27]. This process is also associated with rock salt, since gypsum-containing rock formations are effectively infiltrated and resolved [52–54].

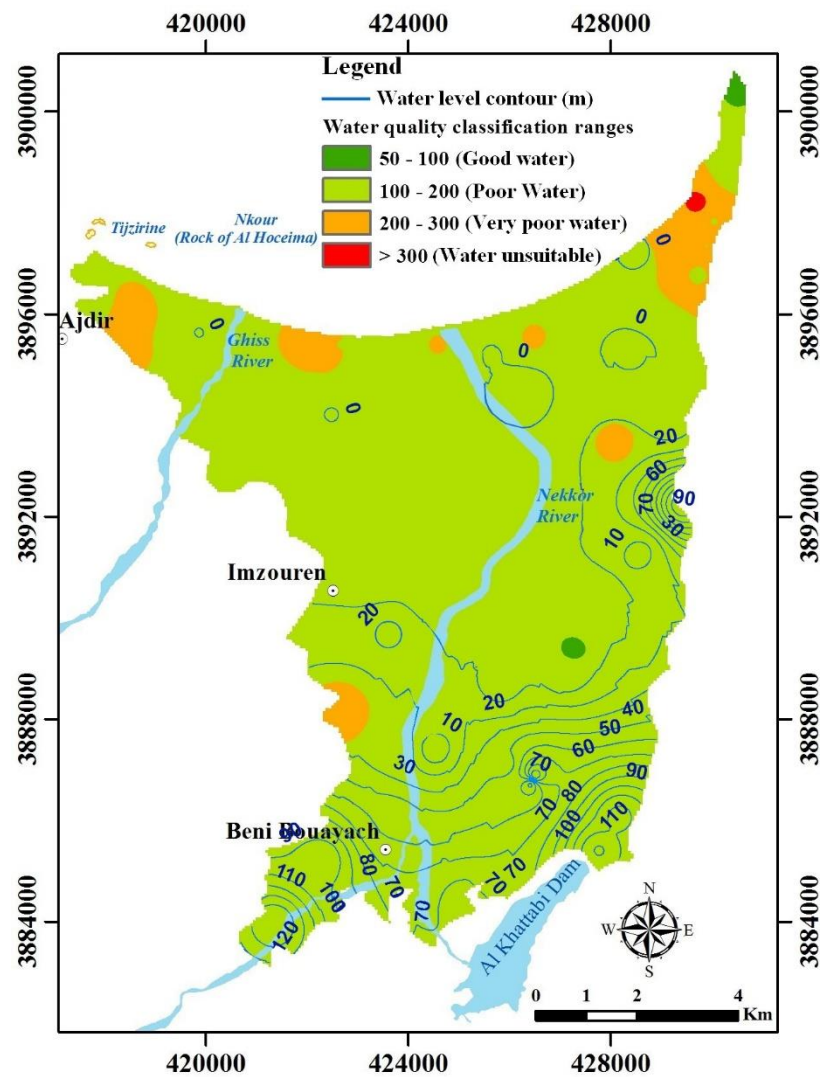


Figure 5. Water quality classification ranges.

Table 3. WQI-based water quality categorization ranges and water types in the Ghiss-Nekkor aquifer.

Range	Type of Water	No. of Samples	Values in %
<50	Excellent water	-	-
50–100	Good water	36	6%
100–200	Poor water		72%
200–300	Very poor water	10	20%
>300	Water unsuitable for drinking purposes	1	2%

Furthermore, based on Supplemental Table 1, the spatial classification of WQI for groundwater of the Ghiss-Nekkor aquifer is presented in Figure 5, showing associations with high restrictions and low restrictions.

### 3.2. Groundwater Quality for Irrigation

The risks related to salinity and sodium are used to determine the appropriateness of water quality for irrigation. The sodium adsorption ratio (SAR) is also used as an index of seawater intrusion. Only the electrical conductivity, sodium percentage (Na%), and sodium adsorption ratio are also used to determine the appropriateness of surface water and groundwater for irrigation use [55].

The SAR is a popular measure of water's suitability to satisfy irrigation requirements. It is calculated using the concentrations of the primary alkaline and alkaline earth cations contained in the water [56,57].

In developing plant growth, the sodium adsorption ratio serves an important role. It estimates the sodium replacement level with other ions' content in the soil, resulting in sodium danger.

These variables form a basis for USSL [58,59] classification charts to assess water quality. Equation (6) is used to determine it; all concentrations are given in milliequivalents/liter:

$$\text{SAR} = \frac{\text{Na}^+}{\sqrt{\text{Ca}^{2+} + \text{Mg}^{2+}}} \quad (6)$$

This represents the SAR values as a function of the electrical conductivity EC in ( $\mu\text{S}/\text{cm}$ ). Thus, the water quality can be classified into 16 classes. Primarily, this can be categorized into four subzones based on the salinity risk.

Low ( $\text{EC} < 250$ ), medium ( $250 < \text{EC} < 750$ ), high ( $750 < \text{EC} < 2250$ ), and very high ( $\text{EC} > 2250$ ) values of salinity are assigned to Class 1 (low salinity hazard), Class 2 (medium salinity hazard), Class 3 (high salinity hazard), and Class 4 (very high salinity hazard), regarded as good, moderate, poor, and very poor water classifications, respectively; secondly, the sodium hazard (vertical axis) is partitioned according to four classes: water that is excellent ( $\text{S1} < 10$ ), good ( $\text{S2}: 10\text{--}18$ ), doubtful ( $\text{S3}: 18\text{--}26$ ), and unsuitable for utilization ( $\text{S4}: > 26$ ), in which the SAR levels are less than 10, between 10 and 18, between 18 and 26, and more than 26, respectively (USSL, 1954).

The plot of electrical conductivity and SAR infers that 4.11% of samples fall in the C3-S1 class, which is generally considered not suitable for irrigation and reveals high-salinity (C3) with low sodium hazard water (S1) (Figure 6). Approximately 9.59% of the samples fall into the high salinity class (C4-S1), corresponding to a very high SAR that is regarded as not eligible for irrigation. About 79.45% of the sample results fall within the alkali risk category with very high salinity and alkali (C4-S2), and the rest of the samples, which represents a percentage of 6.85%, fall into the zones of C4S3 to C4S4, such as inferior water quality for irrigating plants through high tolerance to salt alone.

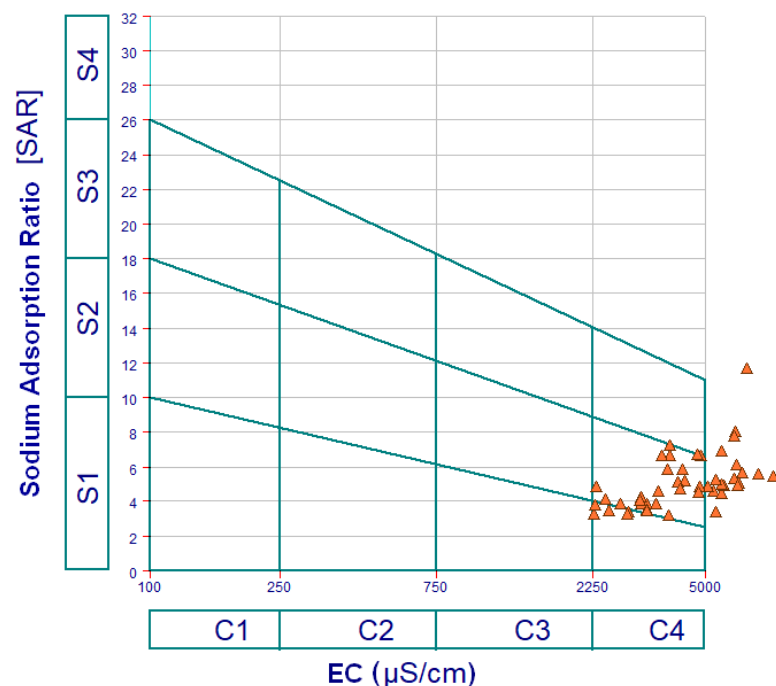


**Figure 6.** USSL salinity diagram for SAR and EC classification of irrigation waters as defined by Richards (1968) [58].

In addition, the Wilcox classification [59] graph is based on the percentage of soluble sodium (Na%). It is also applied to assess the quality of groundwater and its suitability for use in irrigation [60,61]. Groundwater in the study area is doubtful and unsuitable for irrigation (Figure 7). This figure divides water quality appropriateness into five zones: excellent to good, good to permissible, permissible to questionable, doubtful to unsuitable, and unsuitable for irrigation. A Na% content of more than 60% in water causes an accumulation of sodium and, thus, leads to a deterioration of the physical properties of the soil [62,63]. The following formula is used to determine sodium percentages (Singh and Kumar 2015), where all concentrations are expressed in milliequivalents:

$$\% \text{Na} = \frac{\text{Na}^+}{\text{Na}^+ + \text{K}^+ + \text{Ca}^{2+} + \text{Mg}^{2+}} \times 100 \quad (7)$$

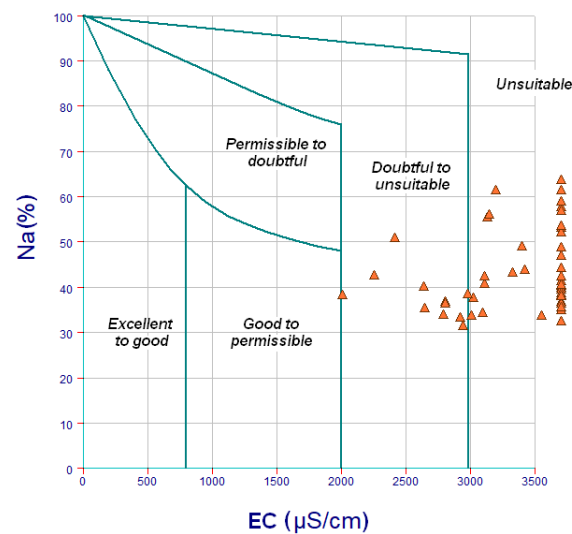


Figure 7. Wilcox diagram indicating groundwater suitability for irrigation [59].

Na% varied from 31.06% to 63.18%, with an average value of 42.37%. Some of the samples (18%) have Na% values ranging from 32.93% to 49.48%, which fall into the doubtful to unsuitable class. Therefore, around 82% of the samples are classified as unfit for irrigation water use, as shown in Figure 7 (Supplementary Table S4). This results from seawater intrusion, especially near the coastal fringe, causing an excessive sodium percentage. Therefore, it can be associated with pollution from urban and industrial activities [33]. Also, irrigation water use and the significant result of high electrical conductivity (Figure 3) decrease plant osmotic activity, interfering with overall nutrient and water absorption from the soil. In addition, according to a Moroccan water quality report, groundwater quality in the Ghiss-Nekkor aquifer was categorized as poor to very poor based on the conductivity problem [64].

$$\text{SC} = (\text{CO}_3^{2-} + \text{HCO}_3^-) - (\text{Ca}^{2+} + \text{Mg}^{2+}) \quad (8)$$

Residual Sodium Carbonate (RSC) is an important criteria for identifying the impact of  $\text{HCO}_3^-$  and  $\text{CO}_2$  on irrigation quality [65,66]. RSC is applied as an indicator of the soil alkalinity risk [67]. The residual sodium carbonate index (RSC) is obtained by Equation (8) [68]. Groundwater in the study area presents RSC values varying from  $-30.74$  to  $-4.61 \text{ meq}\cdot\text{dm}^{-3}$ , with an average of  $-16.78 \text{ meq}\cdot\text{dm}^{-3}$  (Table 1).

$$\text{PI} = \frac{(\text{Na} + \sqrt{\text{HCO}_3})}{(\text{Ca} + \text{Mg} + \text{Na})} 100 \quad (9)$$

Furthermore, the permeability index (PI) is another indicator used to assess water suitability for irrigation, which evaluates the efficiency of water flux (permeability) in the

soil system and assesses the quality of groundwater for irrigation using ions in units of milliequivalents per liter [69].

### 3.3. Groundwater Quality for Drinking

To assess the Ghiss-Nekkor aquifer's drinking water quality, we plotted the chemical analysis results of the water samples on a Schuler graph (Figure 8), which brought in the high sulfate ion. According to this diagram, the quality parameters change throughout different years; electrical conductivity, TDS, chlorate, and bicarbonate water richness reveal the total hardness. Based on this diagram, the amounts of chloride, sodium, total hardness, and sulfate have increased, which is unsuitable for consumption by humans.

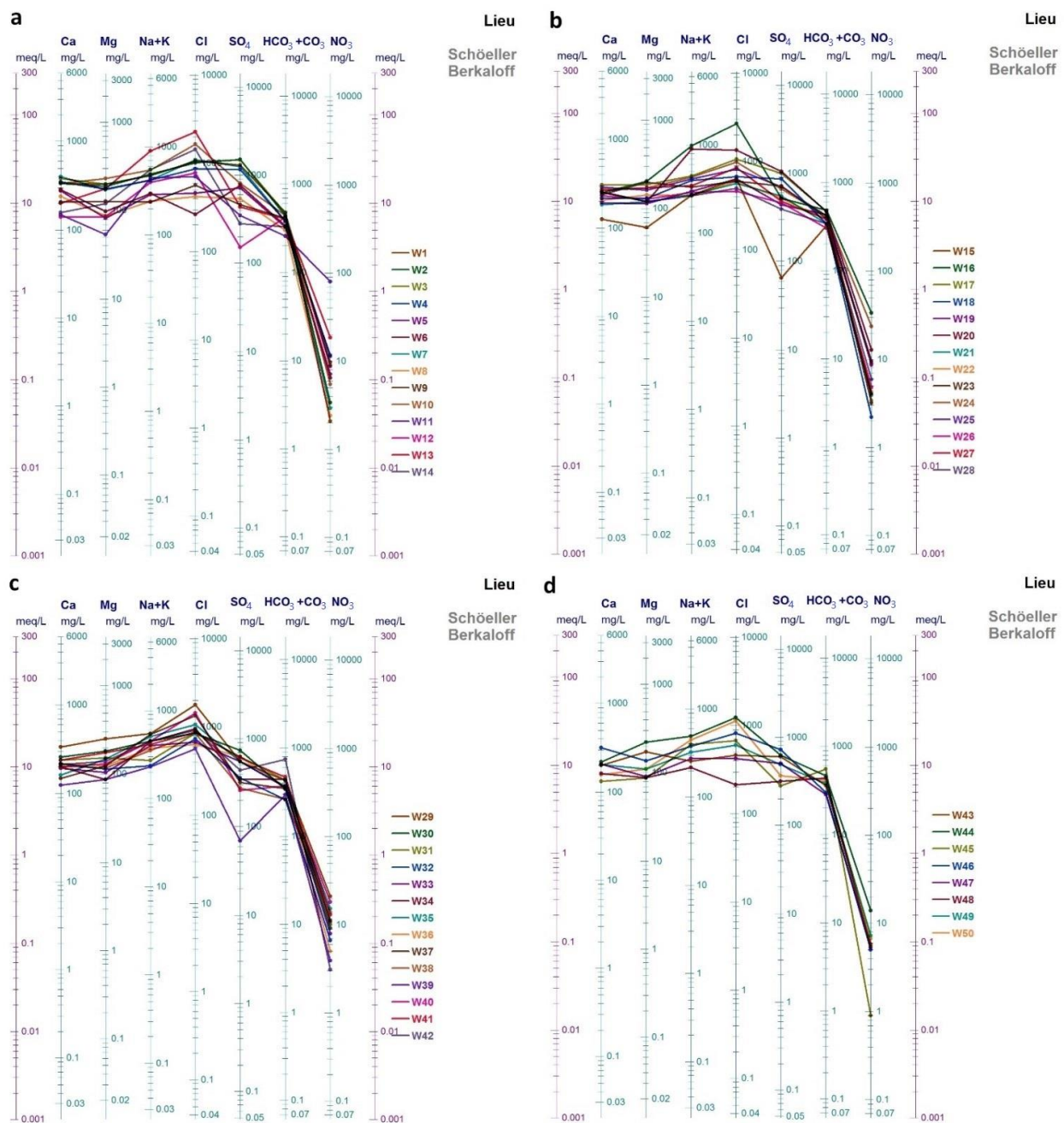


**Figure 8.** Groundwater category of the Ghiss-Nekkor aquifer (Schuler diagram), (a) Samples from well number 1 to 14, (b) Samples from well number 15 to 28, (c) Samples from well member 29 to 42, (d) Samples from well member 43 to 50.

### 3.4. Statistical Analysis

Principal component analysis (PCA) is used to obtain correlations and complete information of variables and observation sites in hydrochemistry investigations.

Moreover, Supplemental Table S2 shows a positive correlation between TDS and  $\text{Na}^+$ , which are significantly correlated. This indicates the involvement of this ion in the mineralization acquisition of groundwater [70,71]. The combination of TDS and  $\text{Na}^+$  ion is beneficial in explaining hydrochemical processes. Groundwater samples with increased TDS values (Figure 3) indicate the existence of leaching and dissolution processes from marine source deposits and mixing with seawater [72]; in addition, the salinity of the Ghiss-Nekkor aquifer samples is probably attributed to seawater intrusion [34]. These high values are generally not allowed for human consumption (WHO, 2011), as  $\text{TDS} > 2000 \text{ mg/L}$  values are deleterious to many crops and plants [73]. Bromide generally increases in concentration from upstream to the sea. This parameter's ions show a majority decrease from the mixing line, suggesting that this component is provided by the evaporation process via the mixing of seawater and freshwater.

The calcium element ( $\text{Ca}^{2+}$ ) at concentrations ranging from 124.25 to 400.80 mg/L (Figure 3) has very low values from the southwest (Beni Bouayach) to the northeast (Azrar) and high values from the northwest (Imzouren) to the north (Ait Youssef Ou Ali). Magnesium contents vary from 53.76 to 254.00 mg/L, with an average of 140.37 mg/L (Figure 3), and the highest concentrations are in the Sfiha, Ait Youssef Ou Ali, Azrar, and Trougout areas.

Sodium, sulfate, magnesium, potassium, and calcium values mean the strong influence of all these ions in mineralization processes (Supplementary Table S2).

A correlation coefficient is a popular tool for determining and measuring the relationship between two variables. It is an essential statistical tool that indicates the degree of dependence of one variable on another. PCA was applied to the 50 samples.

Based on two factors (F1 and F2), we reinforced the perceived trends and classified the variables as four distinct groups (Figure 9a).  $\text{Na}^+$ ,  $\text{Mg}^{2+}$ ,  $\text{Cl}^-$ , EC, WQI, and total dissolved solids (TDS) composed the first correlation group, while  $\text{SO}_4^{2-}$  and  $\text{Ca}^{2+}$  formed the second group. The third correlation group included  $\text{HCO}_3^-$ , and the fourth correlation group contained  $\text{K}^+$ ,  $\text{NO}_3^-$ , and  $\text{Br}^-$ .

The diagram of factors (Figure 9a) shows the mineralization processes. In the first case, the groundwater is enriched with Na and Cl ions [74]. Secondly, a dissolution effect of carbonates and evaporites coupled with a production of  $\text{HCO}_3^-$  occurs (Figure 3). This assemblage indicates the mineralization associated with water–rock contact and anthropogenic activity (household and agriculture). Eventually, chlorides in the Ghiss-Nekkor plain may have various sources, including leaching from sedimentary soils, saltwater intrusion, domestic and industrial waste discharges, rock alteration, etc. [75].

The results suggest that the first component (Axis 1) accounts for 42.50% (Figure 9b) of the total variance. This percentage shows the highly mineralized character of the groundwater. A high value is observed in the wells (10, 13, 16, 20, and 29). This percentage shows the highly mineralized character of the groundwater and is strongly related to electrical conductance. In general, this percentage is explained within this axis. This percentage is explained by this axis having a dominant positive charge for  $\text{Na}^+$ ,  $\text{Cl}^-$ , and EC; thus, it could probably denote the dissolution of the sedimentary and evaporite rocks present in the Ghiss-Nekkor aquifer [74]. Therefore, this component is indicative of the signature of a natural recharge and the water–rock interaction process.

The second factor (Axis 2) accounts for only 12.92% of the total variance, containing a majority of  $\text{K}^+$ ,  $\text{NO}_3^-$ ,  $\text{Br}^-$ ,  $\text{SO}_4^{2-}$ , and  $\text{Ca}^{2+}$ , which provides an indication of anthropogenic activities and their influence on the Ghiss-Nekkor aquifer, mainly related to organic matter and chemical fertilizers. Thus, the lack of collection, evacuation, and treatment of wastewater and household waste, as well as defecation in natural areas and the infiltration of organic matter into soil, are, therefore, the factors that can explain why water is polluted. Other contributing factors include the infiltration of organic matter into soil. Also,

the generation of  $\text{NO}_3^-$  from nitrification processes is related to releasing  $\text{H}^+$  ions into the solution.

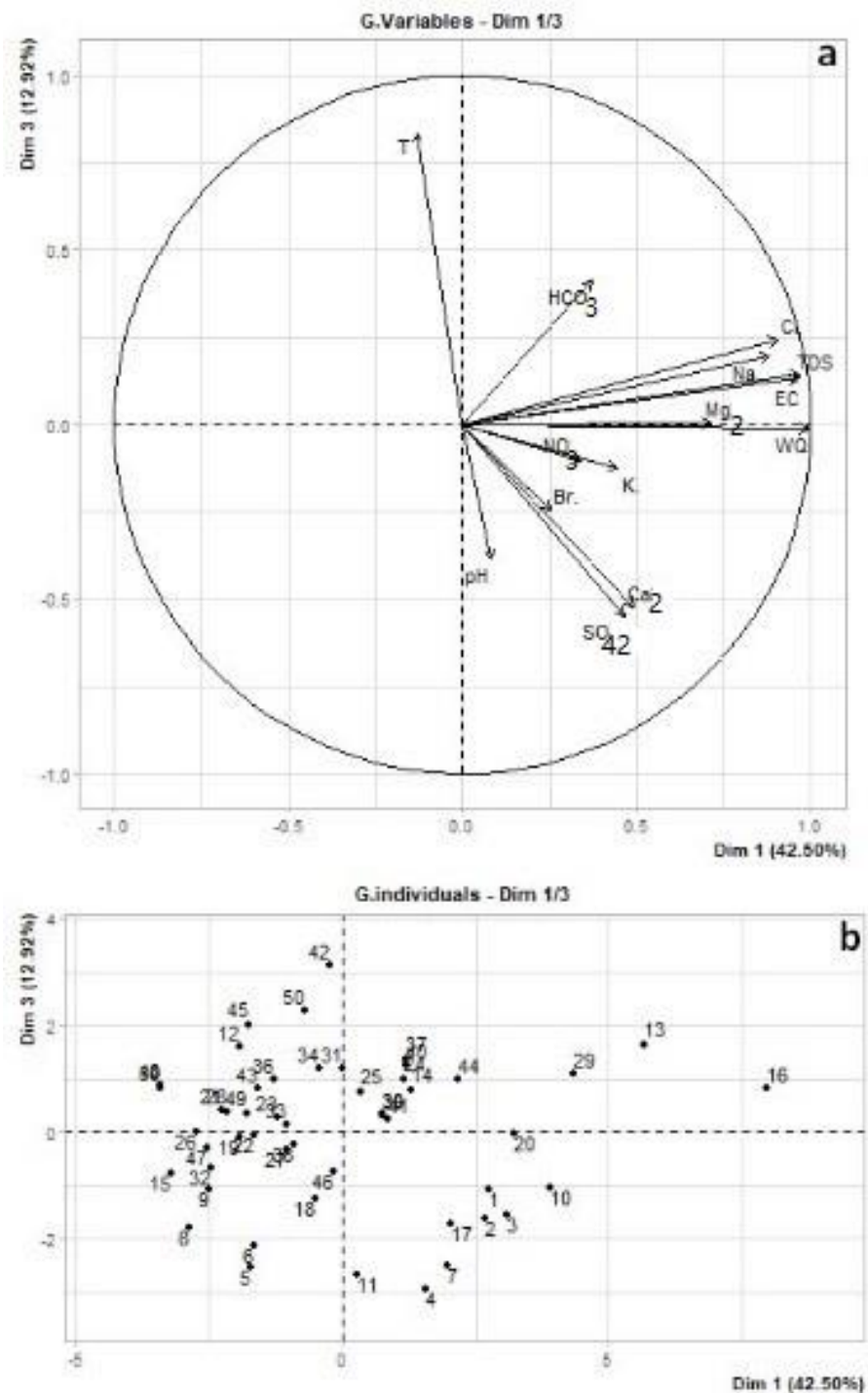


**Figure 9.** PCA loadings of the 50 experimental (a) variables of the F1/F2 factorial plan and (b) graphical illustration of the groundwater and hydrochemical parameters of the Ghiss-Nekkor aquifer in the space of the axes (F1–F2).

### 3.5. Analysis of Artificial Neural Network

In this study, we used the Broyden–Fletcher–Goldfarb–Shannolbgfs (BFGS) training algorithm to obtain the weights of the MLP model and the hyperbolic tangent linear as activation functions for the hidden and output layers, respectively. The number of

hidden neurons was determined by trying different values between 2 and 50. With 20 buried neurons, the most significant results were achieved. Python 3.8 and the sci-kit-learn module were used to create all the simulations. The outcomes from both training and testing are shown in Table 4.

**Table 4.** Statistical regression parameters for the preferred result (MLP<sub>BFGS</sub> WQI).

	R <sup>2</sup>		RMSE		MAE	
	Training	Test	Training	Test	Training	Test
MLP	0.9903	0.9885	5.1746	5.8031	4.0804	4.7211

This reveals the RMSE and MAE values increased during the testing phase by 12.14% and 15.7%, respectively. However, the R<sup>2</sup> decreased slightly by 1.8%. Figure 10 illustrates the regression plots between the measured and the predicted WQI values per the MLP model. As can be seen from this figure, the MLP model showed a high correlation between observed and estimated values, with values of R<sup>2</sup> = 0.9903 and R<sup>2</sup> = 0.9885 for the training and testing processes, respectively (Figure 10). These findings show the robustness of the MLP approach for predicting WQI.

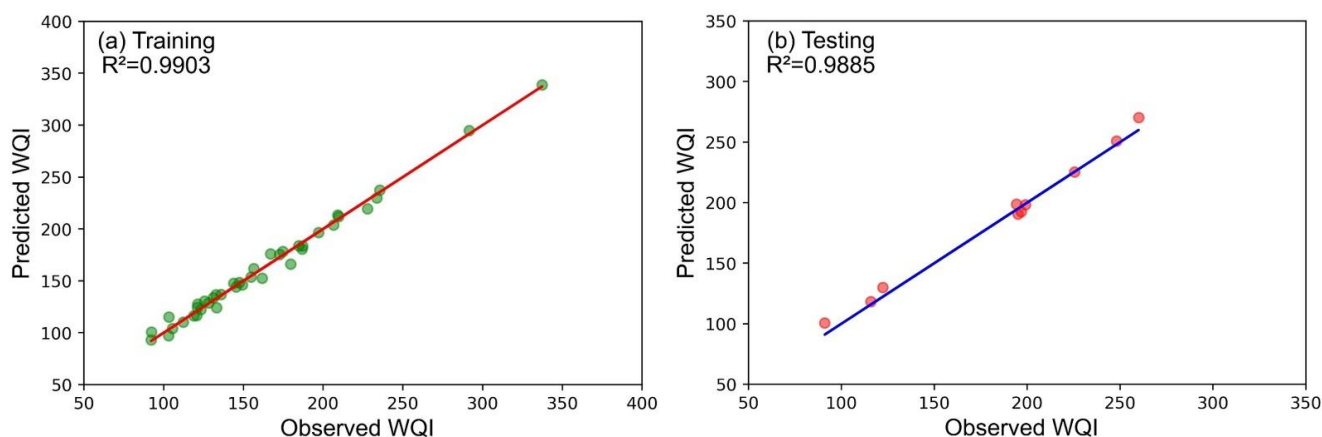


**Figure 10.** Plot of prediction versus ANN test data.

Water demand is considerably increasing, while the groundwater of Ghiss-Nakker supplies much of the rural population. For this reason, it is necessary to apply monitoring and control its quality, in order to detect the sources of pollution and to look for adequate solutions to minimize the effect of pollution on the groundwater.

The advantages of this study are to apply the statistical and descriptive analyses to the physico-chemical data for the management and control of water quality at the Ghiss-Nekkor aquifer and to visualize and analyze the existing correlations between the different variables through their structuring and their orientations, to identify the main factors responsible for the quality of the water found during the sampling season [76].

According to the results obtained, the high degree of mineralization is probably linked to the substrate types crossed by the groundwater and reinforced by the infiltration of rainfall and surface water [73]. In addition, the hypothesis of this study focused only on groundwater quality analyses. Consequently, the government's 200 water managers should look for new technologies, models, and methods to monitor water quality. To put efficient measures for the protection of the environment into place, first a method for the ongoing monitoring of the groundwater must be set up to reduce the amounts of the contaminating factors, such as salinity. Consequently, the salinity reflects that the majority of wells currently have a total of more than 2 g/L [34]

Previously, [74] studied the assessment of the impact of Imzouren's WWTP on the quality of the surrounding groundwater, in the central Rif (northern Morocco). Their

results showed that the pollution of the wells studied were characterized by salinization phenomena and very mineralized. The results of a study conducted by [77] in regions of the Rif found that the water from the wells in the Ben Taib region did not significantly exceed Moroccan or world standards.

Our study provides a good example for the treatment of data from a groundwater highly loaded with organic and mineral pollutants. For most of the parameters measured in the samples, the recorded values were very high.

#### 4. Conclusions

According to several physicochemical parameters, the results reveal significant variations in the groundwater's major ions and salinity in the Ghiss-Nekkor aquifer, Al Hoceima, Morocco. More than half of the samples exceeded the statistically allowable potability limits for EC, Na<sup>+</sup>, and Cl<sup>-</sup>. Based on statistical analysis, the variables affecting the groundwater chemistry in the Ghiss-Nekkor aquifer included soil and rock alteration and evaporation, revealing the dissolution of evaporated minerals in the groundwater flow path. The conclusion can be derived from the result of the sodium adsorption ratio (SAR), Schuler diagram, Wilcox plot, and the percentage of sodium (Na%), in which the majority of the samples were unsuitable for irrigation purposes, and the salinity of these samples can probably be assigned to seawater intrusion. Additionally, the RSC reported a medium-to-high risk of alkalinity caused by an elevated HCO<sub>3</sub><sup>-</sup> concentration.

Also, this study forecasted water quality by lowering the parameters without losing any information. For the prediction of the WQI, the MLR approach was used. The input variable in the ANN showed 12 parameters, which had the highest prediction performance among others. The results showed that the MLP model could predict WQI with high accuracy. Furthermore, the WQI revealed that groundwater resources in the Ghiss-Nekkor aquifer are inadequately managed, with more than 80% referred to as "poor water". This is due to various reasons, including overexploitation, harsh weather conditions, saltwater intrusion, and an insufficient regeneration capacity of groundwater. A Bland–Altman test confirmed the model's appropriateness. The findings revealed that 50 samples (98.85%) fell inside the confidential threshold, indicating that the ANN-generated model may be used as an alternate option if physical and chemical analyses cannot be conducted with 99.0% accuracy. This is the first study to construct an ANN prediction model for the WQI of the Ghiss-Nekkor. Future research could focus on other factors that influence ANNs' predictive output to find the most accurate model. Comparative studies of prediction models might also be helpful.

**Supplementary Materials:** The following supporting information can be downloaded at: <https://www.mdpi.com/article/10.3390/su15010402/s1>.

**Author Contributions:** Conceptualization, Y.E.Y., M.H. and H.E.O.; methodology, Y.E.Y., M.H., H.G., A.A. and N.E.; software, Y.E.Y., M.H., H.E.O., A.E. (Ali Essahlaouiand), S.H. and N.E.; validation, Y.E.Y., M.H., H.G., A.A. and M.Z.; formal analysis, Y.E.Y., M.H. and H.E.O.; investigation, Y.E.Y., M.H., H.G. and A.A.; resources, Y.E.Y., M.H., H.E.O., H.G., A.A. and M.A.; data curation, Y.E.Y., M.H., H.E.O. and S.B.; writing—original draft preparation, Y.E.Y.; writing—review and editing, Y.E.Y., M.H., H.G., A.A., M.A., S.B., N.E., H.A.H., A.E. (Abdallah Elaaraj) and M.C.; visualization, Y.E.Y., M.H., H.G. and A.A.; supervision, M.H. and H.E.O.; project administration, Y.E.Y., M.H. and H.E.O.; funding acquisition, M.H. and H.E.O. All authors have read and agreed to the published version of the manuscript.

**Funding:** This research received no external funding.

**Institutional Review Board Statement:** Not applicable.

**Informed Consent Statement:** Not applicable.

**Data Availability Statement:** Not applicable.

**Acknowledgments:** This project was performed as part of the Moroccan MENESFCRS-funded research project PPR2 "Biodiversity and Groundwater Quality in the Al Hoceima Region (Northern

Morocco): Application to Hygiene, Monitoring, and Aquifer Protection". We also thank the anonymous reviewers and the editor for their useful and constructive comments and suggestions that greatly contributed to the improvement of the form and quality of the manuscript.

**Conflicts of Interest:** The authors declare no conflict of interest.

## References

1. Kazakis, N.; Mattas, C.; Pavlou, A.; Patrikaki, O.; Voudouris, K. Multivariate Statistical Analysis for the Assessment of Groundwater Quality under Different Hydrogeological Regimes. *Environ. Earth Sci.* **2017**, *76*, 349. [[CrossRef](#)]
2. WHO (World Health Organization). *Guidelines for Drinking-Water Quality: First Addendum to the Fourth Edition*; World Health Organization: Geneva, Switzerland, 2017; ISBN 9789241549950.
3. Bharti, P.K.; Chauhan, A. *Environmental Biotechnology and Application*; Discovery Publishing House: New Delhi, India, 2013.
4. Gueddari, H.; Akodad, M.; Baghour, M.; Moumen, A.; Skalli, A.; El Yousfi, Y.; Ait Hmeid, H.; Chahban, M.; Azizi, G.; Rahhou, A.; et al. Assessment of the Metal Contamination Index in Groundwater of the Quaternary of the Middle Kert Basin, North-Eastern Morocco. *Environ. Qual. Manag.* **2021**, *32*, 53–62. [[CrossRef](#)]
5. Jayaswal, K.; Sahu, V.; Gurjar, B.R. Water Pollution, Human Health and Remediation. In *Water Remediation; Energy, Environment, and Sustainability*; Springer: Berlin/Heidelberg, Germany, 2018; pp. 11–27. [[CrossRef](#)]
6. Mahmoodabadi, M.; Rezaei Arshad, R. Long-Term Evaluation of Water Quality Parameters of the Karoun River Using a Regression Approach and the Adaptive Neuro-Fuzzy Inference System. *Mar. Pollut. Bull.* **2018**, *126*, 372–380. [[CrossRef](#)] [[PubMed](#)]
7. Busico, G.; Kazakis, N.; Cuoco, E.; Colombani, N.; Tedesco, D.; Voudouris, K.; Mastrocicco, M. A Novel Hybrid Method of Specific Vulnerability to Anthropogenic Pollution Using Multivariate Statistical and Regression Analyses. *Water Res.* **2020**, *171*, 115386. [[CrossRef](#)] [[PubMed](#)]
8. Li, P.; Qian, H.; Howard, K.W.; Wu, J. Building a New and Sustainable "Silk Road Economic Belt". *Environ. Earth Sci.* **2015**, *74*, 7267–7270. [[CrossRef](#)]
9. Singha, S.; Pasupuleti, S. Delineation of Groundwater Prospect Zones in Arang Block, Raipur District, Chhattisgarh, Central India, Using Analytical Network Process. *J. Geol. Soc. India* **2020**, *95*, 609–615. [[CrossRef](#)]
10. Singha, S.S.; Pasupuleti, S. Hydrogeochemical Modeling Based Approach for Evaluation of Groundwater Suitability for Irrigational Use in Korba District, Chhattisgarh, Central India. *SN Appl. Sci.* **2020**, *2*, 1551. [[CrossRef](#)]
11. Alitane, A.; Essahlaoui, A.; Van Griensven, A.; Yimer, E.A.; Essahlaoui, N.; Mohajane, M.; Chawanda, C.J.; Van Rompaey, A. Towards a Decision-Making Approach of Sustainable Water Resources Management Based on Hydrological Modeling: A Case Study in Central Morocco. *Sustainability* **2022**, *14*, 10848. [[CrossRef](#)]
12. Garewal, S.K.; Vasudeo, A.D.; Landge, V.S.; Ghare, A.D. A GIS-Based Modified DRASTIC (ANP) Method for Assessment of Groundwater Vulnerability: A Case Study of Nagpur City, India. *Water Qual. Res. J.* **2017**, *52*, 121–135. [[CrossRef](#)]
13. Brown, R.M.; McClelland, N.I.; Deininger, R.A.; Tozer, R.G. A Water Quality Index: Do We Dare? *Work. Water Sew.* **1970**, *117*, 339–343.
14. Singha, S.; Pasupuleti, S.; Singha, V.G.K.V. An Integrated Approach for Evaluation of Groundwater Quality in Korba District, Chhattisgarh Using Geomatic Techniques. *J. Environ. Biol.* **2017**, *38*, 865. [[CrossRef](#)]
15. Banerji, S.; Mitra, D. Geographical Information System-Based Groundwater Quality Index Assessment of Northern Part of Kolkata, India for Drinking Purpose. *Geocarto Int.* **2019**, *34*, 943–958. [[CrossRef](#)]
16. Abbasnia, A.; Yousefi, N.; Mahvi, A.H.; Nabizadeh, R.; Radfard, M.; Yousefi, M.; Alimohammadi, M. Evaluation of Groundwater Quality Using Water Quality Index and Its Suitability for Assessing Water for Drinking and Irrigation Purposes: Case Study of Sistan and Baluchistan Province (Iran). *Hum. Ecol. Risk Assess.* **2019**, *25*, 988–1005. [[CrossRef](#)]
17. Ribeiro, L.; Paralta, E.; Nascimento, J.; Amaro, S.; Oliveira, E. A Agricultura e a Delimitação Das Zonas Vulneráveis Aos Nitratos de Origem Agrícola Segundo a Directiva 91/676/Ce. 2002. Available online: [Ce.grupo.us.es/ciberico/archivos\\_acrobat/sevilla3ribeiro.pdf](http://Ce.grupo.us.es/ciberico/archivos_acrobat/sevilla3ribeiro.pdf) (accessed on 15 October 2022).
18. Hsu, K.; Gupta, H.V.; Adamowski, J.; Fung Chan, H.; Prasher, S.O.; Ozga-Zielinski, B.; Sliusarieva, A. Artificial Neural Network Modeling of the Rainfall-Runoff Process That Arise and Based Background and Scope. *Water Resour. Res.* **1995**, *48*, 1–14.
19. Maier, H.R.; Dandy, G.C. Neural Networks for the Prediction and Forecasting of Water Resources Variables: A Review of Modelling Issues and Applications. *Environ. Model. Softw.* **2000**, *15*, 101–124. [[CrossRef](#)]
20. Coulibaly, P.; Anctil, F.; Aravena, R.; Bobée, B. Artificial Neural Network Modeling of Water Table Depth Fluctuations. *Water Resour. Res.* **2001**, *37*, 885–896. [[CrossRef](#)]
21. Mohanty, S.; Jha, M.K.; Kumar, A.; Panda, D.K. Comparative Evaluation of Numerical Model and Artificial Neural Network for Simulating Groundwater Flow in Kathajodi-Surua Inter-Basin of Odisha, India. *J. Hydrol.* **2013**, *495*, 38–51. [[CrossRef](#)]
22. Tokatli, C. Drinking Water Quality Assessment of Ergene River Basin (Turkey) by Water Quality Index: Essential and Toxic Elements. *Sains Malays.* **2019**, *48*, 2071–2081. [[CrossRef](#)]
23. Štambuk-Giljanović, N. Water Quality Evaluation by Index in Dalmatia. *Water Res.* **1999**, *33*, 3423–3440. [[CrossRef](#)]
24. Aliyu, A.G.; Jamil, N.R.B.; Adam, M.B.B.; Zulkeflee, Z. Spatial and Seasonal Changes in Monitoring Water Quality of Savanna River System. *Arab. J. Geosci.* **2020**, *13*, 55. [[CrossRef](#)]

25. Mishra, A.P.; Singh, S.; Jani, M.; Singh, K.A.; Pande, C.B.; Varade, A.M. Assessment of Water Quality Index Using Analytic Hierarchy Process (AHP) and GIS: A Case Study of a Struggling Asan River. *Int. J. Environ. Anal. Chem.* **2022**, 1–13. [[CrossRef](#)]
26. Lanjwani, M.F.; Khuhawar, M.Y.; Jahangir Khuhawar, T.M.; Lanjwani, A.H.; Soomro, W.A. Evaluation of Hydrochemistry of the Dokri Groundwater, Including Historical Site Mohenjo-Daro, Sindh, Pakistan. *Int. J. Environ. Anal. Chem.* **2021**, 1–25. [[CrossRef](#)]
27. Nouayti, N.; Cherif, E.K.; Algarra, M.; Pola, M.L.; Fernández, S.; Nouayti, A.; Esteves da Silva, J.C.; Driss, K.; Samlani, N.; Mohamed, H. Determination of Physicochemical Water Quality of the Ghis-Nekor Aquifer (Al Hoceima, Morocco) Using Hydrochemistry, Multiple Isotopic Tracers, and the Geographical Information System (GIS). *Water* **2022**, *14*, 606. [[CrossRef](#)]
28. Chafouq, D.; El Mandour, A.; Elgettafi, M.; Himi, M.; Choukri, I.; Casas, A. Hydrochemical and Isotopic Characterization of Groundwater in the Ghis-Nekor Plain (Northern Morocco). *J. Afr. Earth Sci.* **2018**, *139*, 1–13. [[CrossRef](#)]
29. Elgettafi, M.; Elmeknassi, M.; Elmandour, A.; Himi, M.; Lorenzo, J.M.; Casas, A.  $\Delta 34S$ ,  $\Delta 18O$ , and  $\Delta 2H$ - $\Delta 18O$  as an Approach for Settling the Question of Groundwater Salinization in Neogene Basins: The North of Morocco in Focus. *Water* **2022**, *14*, 3404. [[CrossRef](#)]
30. d’Acremont, E.; Gutscher, M.-A.; Rabaute, A.; de Lépinay, B.M.; Lafosse, M.; Poort, J.; Ammar, A.; Tahayt, A.; Le Roy, P.; Smit, J. High-Resolution Imagery of Active Faulting Offshore Al Hoceima, Northern Morocco. *Tectonophysics* **2014**, *632*, 160–166. [[CrossRef](#)]
31. Booth-Rea, G.; Jabaloy-Sánchez, A.; Azdimousa, A.; Asebriy, L.; Vílchez, M.V.; Martínez-Martínez, J.M. Upper-Crustal Extension during Oblique Collision: The Tamsamani Extensional Detachment (Eastern Rif, Morocco). *Terra Nova* **2012**, *24*, 505–512. [[CrossRef](#)]
32. Kouz, T.; Cherkaoui Dekkaki, H.; Mansour, S.; Hassani Zerrouk, M.; Mourabit, T. Application of GALDIT Index to Assess the Intrinsic Vulnerability of Coastal Aquifer to Seawater Intrusion Case of the Ghiss-Nekor Aquifer (North East of Morocco). In *Groundwater and Global Change in the Western Mediterranean Area*; Springer: Berlin/Heidelberg, Germany, 2018; pp. 169–177.
33. Salhi, A. Géophysique, Hydrogéologie et Cartographie de La Vulnérabilité et Du Risque de Pollution de l’aquifère de Ghis-Nekor (Al Hoceima, Maroc). Ph.D. Thesis, Université Abdelmalek Essaadi, Tétouan, Morocco, 2008.
34. El Yousfi, Y.; Himi, M.; El Ouarghi, H.; Elgettafi, M.; Benyoussef, S.; Gueddari, H.; Aqnouy, M.; Salhi, A.; Alitane, A. Hydrogeochemical and Statistical Approach to Characterize Groundwater Salinity in the Ghiss-Nekkor Coastal Aquifers in the Al Hoceima Province, Morocco. *Groundw. Sustain. Dev.* **2022**, *19*, 100818. [[CrossRef](#)]
35. Rodier, J.; Legube, B.; Merlet, N. *L’analyse de L’eau-10e Éd.*; Dunod: Paris, France, 2016.
36. Domenico, P.A.; Schwartz, F.W. *Physical and Chemical Hydrogeology*; Wiley New York: New York, NY, USA, 1998; Volume 506.
37. Chauhan, A.; Singh, S. Evaluation Of Ganga Water For Drinking Purpose by Water Quality Index At Rishikesh, Uttarakhand, India. *Rep. Opin.* **2010**, *2*, 53–61.
38. Balan, I.; Madan Kumar, P.; Shivakumar, M. An Assessment of Groundwater Quality Using Water Quality Index in Chennai, Tamil Nadu, India. *Chron. Young Sci.* **2012**, *3*, 146. [[CrossRef](#)]
39. Tyagi, S.; Sharma, B.; Singh, P.; Dobhal, R. Water Quality Assessment in Terms of Water Quality Index. *Am. J. Water Resour.* **2020**, *1*, 34–38. [[CrossRef](#)]
40. Imneisi, I.B.; Aydin, M. Water Quality Index (WQI) for Main Source of Drinking Water (Karaçomak Dam) in Kastamonu City, Turkey. *J. Environ. Anal. Toxicol.* **2016**, *6*, 5. [[CrossRef](#)]
41. Li, P.; He, X.; Guo, W. Spatial Groundwater Quality and Potential Health Risks Due to Nitrate Ingestion through Drinking Water: A Case Study in Yan’an City on the Loess Plateau of Northwest China. *Hum. Ecol. Risk Assess.* **2019**, *25*, 11–31. [[CrossRef](#)]
42. Subba Rao, N.; Surya Rao, P.; Venktram Reddy, G.; Nagamani, M.; Vidyasagar, G.; Satyanarayana, N.L.V.V. Chemical Characteristics of Groundwater and Assessment of Groundwater Quality in Varaha River Basin, Visakhapatnam District, Andhra Pradesh, India. *Environ. Monit. Assess.* **2012**, *184*, 5189–5214. [[CrossRef](#)]
43. Zakir, H.M.; Sharmin, S.; Akter, A.; Rahman, M.S. Assessment of Health Risk of Heavy Metals and Water Quality Indices for Irrigation and Drinking Suitability of Waters: A Case Study of Jamalpur Sadar Area, Bangladesh. *Environ. Adv.* **2020**, *2*, 100005. [[CrossRef](#)]
44. Gaikwad, S.K.; Kadam, A.K.; Ramgir, R.R.; Kashikar, A.S.; Wagh, V.M.; Kandekar, A.M.; Gaikwad, S.P.; Madale, R.B.; Pawar, N.J.; Kamble, K.D. Assessment of the Groundwater Geochemistry from a Part of West Coast of India Using Statistical Methods and Water Quality Index. *HydroResearch* **2020**, *3*, 48–60. [[CrossRef](#)]
45. WHO (World Health Organization). *Water Quality for Drinking: WHO Guidelines*; Springer: Berlin/Heidelberg, Germany, 2011. [[CrossRef](#)]
46. Bekkoussa, S.; Bekkoussa, B.; Taupin, J.-D.; Patris, N.; Meddi, M. Groundwater Hydrochemical Characterization and Quality Assessment in the Ghriss Plain Basin, Northwest Algeria. *J. Water Supply Res. Technol.-AQUA* **2018**, *67*, 458–466. [[CrossRef](#)]
47. Bouderbala, A. Assessment of Water Quality Index for the Groundwater in the Upper Chelif Plain, Algeria. *J. Geol. Soc. India* **2017**, *90*, 347–356. [[CrossRef](#)]
48. Sahu, P.; Sikdar, P.K. Hydrochemical Framework of the Aquifer in and around East Kolkata Wetlands, West Bengal, India. *Environ. Geol.* **2008**, *55*, 823–835. [[CrossRef](#)]
49. Yidana, S.M.; Yidana, A. Assessing Water Quality Using Water Quality Index and Multivariate Analysis. *Environ. Earth Sci.* **2010**, *59*, 1461–1473. [[CrossRef](#)]
50. Hastie, T.; Tibshirani, R.; Friedman, J. *The Elements of Statistical Learning*; Springer: Berlin/Heidelberg, Germany, 2009.
51. Computing, S.; Systems, I. *Soft Computing and Intelligent Systems*; Elsevier: Amsterdam, The Netherlands, 2000. [[CrossRef](#)]

52. Huang, P.; Yang, Z.; Wang, X.; Ding, F. Research on Piper-PCA-Bayes-LOOCV Discrimination Model of Water Inrush Source in Mines. *Arab. J. Geosci.* **2019**, *12*, 334. [[CrossRef](#)]
53. Hicham, G.; Mustapha, A.; Mourad, B.; Abdelmajid, M.; Ali, S.; Yassine, E.Y.; Mohamed, C.; Ghizlane, A.; Zahid, M. Assessment of the Physico-Chemical and Bacteriological Quality of Groundwater in the Kert Plain, Northeastern Morocco. *Int. J. Energy Water Resour.* **2021**, *6*, 133–147. [[CrossRef](#)]
54. Zaier, I.; Billiotte, J.; Charmoille, A.; Laouafa, F. The Dissolution Kinetics of Natural Gypsum: A Case Study of Eocene Facies in the North-Eastern Suburbs of Paris. *Environ. Earth Sci.* **2021**, *80*, 8. [[CrossRef](#)]
55. Sappa, G.; Ergul, S.; Ferranti, F.; Sweya, L.N.; Luciani, G. Effects of Seasonal Change and Seawater Intrusion on Water Quality for Drinking and Irrigation Purposes, in Coastal Aquifers of Dar Es Salaam, Tanzania. *J. Afr. Earth Sci.* **2015**, *105*, 64–84. [[CrossRef](#)]
56. Asadollahfardi, G.; Hemati, A.; Moradinejad, S.; Asadollahfardi, R. Sodium Adsorption Ratio (SAR) Prediction of the Halghazi River Using Artificial Neural Network (ANN) Iran. *Curr. World Environ. J.* **2013**, *8*, 169–178. [[CrossRef](#)]
57. Nagaraju, A.; Sunil Kumar, K.; Thejaswi, A. Assessment of Groundwater Quality for Irrigation: A Case Study from Bandalamottu Lead Mining Area, Guntur District, Andhra Pradesh, South India. *Appl. Water Sci.* **2014**, *4*, 385–396. [[CrossRef](#)]
58. McGeorge, W.T. Diagnosis and Improvement of Saline and Alkaline Soils. *Soil Sci. Soc. Am. J.* **1954**, *18*, 348. [[CrossRef](#)]
59. Wilcox, L. *Classification and Use of Irrigation Waters*; US Department of Agriculture: Washington, DC, USA, 1955.
60. Ebraheem, A.M.; Sherif, M.M.; Al Mulla, M.M.; Akram, S.F.; Shetty, A.V. A Geoelectrical and Hydrogeological Study for the Assessment of Groundwater Resources in Wadi Al Bih, UAE. *Environ. Earth Sci.* **2012**, *67*, 845–857. [[CrossRef](#)]
61. Papazotos, P.; Koumantakis, I.; Vasileiou, E. Seawater Intrusion and Nitrate Pollution in Coastal Aquifer of Marathon Basin. *Bull. Geol. Soc. Greece* **2017**, *50*, 927. [[CrossRef](#)]
62. Mtoni, Y.; Mjemah, I.C.; Bakundukize, C.; Van Camp, M.; Martens, K.; Walraevens, K. Saltwater Intrusion and Nitrate Pollution in the Coastal Aquifer of Dar Es Salaam, Tanzania. *Environ. Earth Sci.* **2013**, *70*, 1091–1111. [[CrossRef](#)]
63. Najib, S.; Fadili, A.; Mehdi, K.; Riss, J.; Makan, A.; Guessir, H. Salinization Process and Coastal Groundwater Quality in Chaouia, Morocco. *J. Afr. Earth Sci.* **2016**, *115*, 17–31. [[CrossRef](#)]
64. Mchiouer, F.; Ouarghi, H.E.; Elyousfi, Y.; Abourrich, M. Hygienic quality assessment of well and spring water: A case study of the region of al-hoceima (morocco northern). *Environ. Eng. Manag. J. (EEMJ)* **2022**, *21*, 353–364. [[CrossRef](#)]
65. Eaton, F.M. Significance of Carbonates in Irrigation Waters. *Soil Sci.* **1950**, *69*, 123–134. [[CrossRef](#)]
66. Richards, L.A. *Diagnosis and Improvement of Saline and Alkali Soils*; LWW: Philadelphia, PA, USA, 1954; Volume 78.
67. Al Numanbakhth, M.A.; Howladar, M.F.; Faruque, M.O.; Sohail, M.A.; Rahman, M.M. Understanding the Hydrogeochemical Characteristics of Natural Water for Irrigation Use around the Hard Rock Mine in Maddhapara, Northwest Bangladesh. *Groundw. Sustain. Dev.* **2019**, *8*, 590–605. [[CrossRef](#)]
68. Ragunath, H.M. *Groundwater*, 2nd ed.; Wiley Eastern Ltd.: New Delhi, India, 1987; p. 563.
69. Doneen, L.D. *Notes on Water Quality in Agriculture*; Department of Water Science and Engineering, University of California: Davis, CA, USA, 1964.
70. Mondal, N.C.; Singh, V.P.; Singh, S.; Singh, V.S. Hydrochemical Characteristic of Coastal Aquifer from Tuticorin, Tamil Nadu, India. *Environ. Monit. Assess.* **2011**, *175*, 531–550. [[CrossRef](#)] [[PubMed](#)]
71. Benyoussef, S.; Arabi, M.; El Ouarghi, H.; Ghalit, M.; Azirar, M.; El Midaoui, A.; Ait Boughrou, A. Impact of Anthropogenic Activities on the Quality of Groundwater in the Central Rif (North Morocco). *Ecol. Eng. Environ. Technol.* **2021**, *22*, 69–78. [[CrossRef](#)]
72. Eissa, M.A.; Thomas, J.M.; Pohll, G.; Shouakar-stash, O.; Hershey, R.L.; Dawoud, M. Applied Geochemistry Groundwater Recharge and Salinization in the Arid Coastal Plain Aquifer of the Wadi Watir Delta, Sinai, Egypt. *Appl. Geochem.* **2016**, *71*, 48–62. [[CrossRef](#)]
73. Bauder, T.A.; Waskom, R.M.; Sutherland, P.L.; Davis, J.G.; Follett, R.H.; Soltanpour, P.N. *Irrigation Water Quality Criteria*; Service in Action; No. 0.506; Colorado State University: Fort Collins, CO, USA, 2011.
74. Benyoussef, S.; El Ouarghi, H.; Arabi, M.; El Yousfi, Y.; Azirar, M.; Ait Boughrou, A. Assessment of the Impact of Imzouren City's WWTP on the Quality of the Surrounding Groundwater, at the Rif Central (Northern Morocco). *E3S Web Conf.* **2021**, *240*, 1–4. [[CrossRef](#)]
75. Karanth, K.R. *Ground Water Assessment: Development and Management*; Tata McGraw-Hill Education: New York, NY, USA, 1987.
76. Sadeghfam, S.; Bagheri, A.; Razzagh, S.; Nadiri, A.A.; Vadiati, M.; Senapathi, V.; Sekar, S. Hydrochemical Analysis of Seawater Intrusion by Graphical Techniques in Coastal Aquifers to Delineate Vulnerable Areas. In *Groundwater Contamination in Coastal Aquifers*; Elsevier: Amsterdam, The Netherlands, 2022; pp. 91–104.
77. Gueddari, H.; Akodad, M.; Baghour, M.; Moumen, A.; Skalli, A.; Chahban, M.; Azizi, G.; Hmeid, H.A.; Maach, M.; Riouchi, R. Assessment of Potential Contamination of Groundwater in Abandoned Mining Region of Ben Taieb, Northeastern Morocco Using Statistical Studies. *Int. J. Health Sci.* **2022**, *6*, 4121–4133. [[CrossRef](#)]

**Disclaimer/Publisher's Note:** The statements, opinions and data contained in all publications are solely those of the individual author(s) and contributor(s) and not of MDPI and/or the editor(s). MDPI and/or the editor(s) disclaim responsibility for any injury to people or property resulting from any ideas, methods, instructions or products referred to in the content.